

# Active colloidal particles in emulsion droplets: A model system for the cytoplasm

Viva R. Horowitz<sup>1,2</sup>, Zachary C. Chambers<sup>1</sup>, İrep Gözen<sup>3,4,5,6</sup>, Thomas G. Dimiduk<sup>1</sup>, and  
Vinothan N. Manoharan<sup>\*3,1</sup>

<sup>1</sup>*Department of Physics, Harvard University, Cambridge MA 02138, USA*

<sup>2</sup>*Department of Physics, Hamilton College, Clinton NY 13323 USA*

<sup>3</sup>*Harvard John A. Paulson School of Engineering and Applied Sciences, Harvard University, Cambridge MA 02138 USA*

<sup>4</sup>*Faculty of Medicine, University of Oslo, 0318 Oslo Norway*

<sup>5</sup>*Faculty of Mathematics and Natural Sciences, University of Oslo, 0315 Oslo, Norway*

<sup>6</sup>*Department of Chemistry and Chemical Engineering, Chalmers University of Technology, SE-412 96 Göteborg, Sweden*

June 18, 2018

## Abstract

In living cells, molecular motors create activity that enhances the diffusion of particles throughout the cytoplasm, and not just ones attached to the motors. We demonstrate initial steps toward creating artificial cells that mimic this phenomenon. Our system consists of active, Pt-coated Janus particles and passive tracers confined to emulsion droplets. We track the motion of both the active particles and passive tracers in a hydrogen peroxide solution, which serves as the fuel to drive the motion. We first show that correcting for bulk translational and rotational motion of the droplets induced by bubble formation is necessary to accurately track the particles. After drift correction, we find that the active particles show enhanced diffusion in the interior of the droplets and are not captured by the droplet interface. At the particle and hydrogen peroxide concentrations we use, we observe little coupling between the active and passive particles. We discuss the possible reasons for lack of coupling and describe ways to improve the system to more effectively mimic cytoplasmic activity.

## 1 Introduction

The interior of a biological cell is an active environment driven by the motion of motor proteins. These molecular motors not only transport their cargo, but also enhance the transport of unattached particles in the cytoplasm [1, 2]. The stresses created by the motors cause such particles to diffuse at a rate higher than that expected from thermal fluctuations alone. Indeed, in ATP-depleted cells, the mean-square displacement (MSD) of unattached tracer particles is nearly an order of magnitude smaller than that in untreated cells at lag times of 10 s or more [1], indicating that even particles not directly transported by motors experience an increase in motion. These results suggest that motors play an important role in driving and dispersing a wide range of cellular components.

---

\*vnm@seas.harvard.edu

To better understand how active components can drive unattached, passive particles in confined systems, we study a minimal model for an artificial cell, consisting of colloidal Janus particles and passive particles inside a water-in-oil emulsion droplet. The Janus particles are coated with platinum on one hemisphere, so that they catalyze the breakdown of hydrogen peroxide [3]:



The resulting gradient of dissolved oxygen leads to self-diffusiophoresis [3, 4], providing one mechanism for the Janus particle to move, although self-electrophoresis is likely also important [5]. We observe and track both the active and passive particles to understand how the motions of the two are coupled. As in the cellular system, the activity can be controlled by depleting the system of fuel—in this case, the hydrogen peroxide.

After correcting for drift induced by the production of oxygen bubbles and, to a lesser extent, by sample evaporation, we find that the active particles do show enhanced diffusion in the emulsion droplet, but the passive particles do not diffuse any faster than in the absence of the fuel. The absence of coupling gives insights into what physical considerations may be important for the cell to convert active motion into enhanced diffusion.

## 2 Methods and materials

To make droplets containing Janus particles, tracer particles, and hydrogen peroxide fuel, we first make two batches of dyed polystyrene particles, each with a different dye. One batch is then coated with platinum on one hemisphere to make the Janus particles, and the other becomes the tracer particles. We then mix the particles and encapsulate them in water droplets containing hydrogen peroxide. We use 1- $\mu\text{m}$ -diameter particles in all of our experiments because they are large enough to track easily but small enough that they do not sediment rapidly.

Next, we use fluorescence microscopy to observe the motion of the particles inside the droplet, taking advantage of the different dyes to separate the signals from the Janus and tracer particles. Finally, we track the particles and correct for bulk droplet motion in post-processing. The following subsections give details of each of these steps.

### 2.1 Dying particles

To make both the passive tracer particles and Janus particles, we start with spherical, sulfate polystyrene particles that are 1  $\mu\text{m}$  in diameter (Invitrogen S37498) and fluorescently dye them so that we can distinguish the two types of particles when we eventually put them into droplets. We first wash the particles by centrifuging the solution, removing the supernatant, and replacing it with an equal volume of deionized water (Millipore) five times. We use green fluorescent dye (BODIPY 493/503, Life Technologies, now Thermo Scientific) for the particles that will become the Janus particles and red fluorescent dye (Pyrromethene 650, Exciton) for the tracer particles. In both cases, we saturate a toluene solution with the dye, add 4  $\mu\text{L}$  of dyed toluene to 40  $\mu\text{L}$  of the suspension of particles at 1% w/v, and let the particles swell on a room-temperature tube rotator overnight. We then open the container to atmosphere and allow the toluene to evaporate in a 90°C oven for 12 min. Finally, we wash the particles five times by centrifugation and redispersion in deionized water.

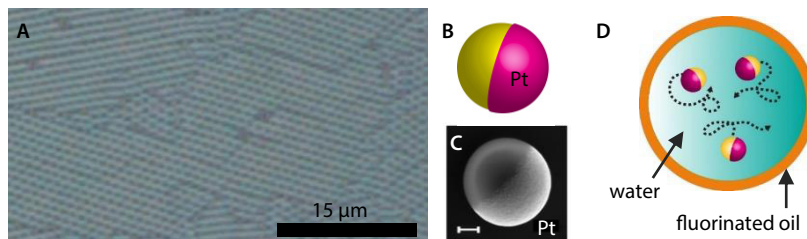


Figure 1: We spread polystyrene sulfate latex microspheres in a monolayer on a glass plate (A: brightfield optical micrograph), then evaporate platinum in a thin layer onto one hemisphere to create Janus particles (B: cartoon of a Janus particle, C: scanning electron micrograph obtained after drop-casting the suspension onto a silicon substrate. Scalebar is 200 nm). D: Simplified cartoon showing the active motion of Janus particles in a water droplet, which is typically 20–80  $\mu\text{m}$  in diameter. Our droplets also contain passive tracer particles, which are not shown here.

## 2.2 Making Janus particles

We make Janus particles by coating half of each particle with a layer of platinum to act as a catalyst for hydrogen peroxide. To do this, we first dilute the suspension of green-dyed particles in ethanol to obtain particles in 50% v/v ethanol/water. We then use a paint drawbar (BYK bar film applicator, item 5552, with a clearance gap of 50.8  $\mu\text{m}$ ) to spread the suspension onto a 4 $\times$ 5-in glass plate, and we let the suspension dry at room temperature, after which we confirm by microscopic inspection that the particles are in a monolayer on the plate (Figure 1A). We then deposit 2 nm titanium (as an adhesion layer) and 10 nm platinum onto the particles on the dried glass plate using an electron-beam evaporator (Denton Explorer). The spherical particles act as their own shadow mask, such that the metal is deposited only onto the top hemisphere of each particle, creating the characteristic two-faced particle (Figure 1B–C).

## 2.3 Making an aqueous suspension of Janus particles

To make the suspension of Janus and tracer particles, we first place the glass plate in a plastic zip-sealed bag filled with deionized water and sonicate it to release the particles, yielding a colloidal suspension of Janus particles in about 1 L of water. We increase the concentration of particles in suspension by centrifuging and removing the supernatant, decreasing the total volume to 2 or 3 mL. To estimate the concentration of the colloidal suspension, we compare microscope images of the Janus particles in water to images of polystyrene particles at 1% w/v and adjust the concentration until the number of particles per volume is approximately matched. We then mix the green Janus particles and red tracer particles in deionized water to obtain a solution with 0.5% w/v tracer particles and a comparable number density of Janus particles. The final, total number density of particles is approximately the same as that of a 1% w/v solution of polystyrene particles. We assume that this number density is the same as that inside the droplets, which are prepared as described below.

## 2.4 Encapsulating Janus particles and tracer particles together in emulsion droplets

We form aqueous droplets containing Janus particles, tracers, and hydrogen peroxide fuel. Timing is a factor in this step because once the peroxide comes into contact with the platinum on the Janus particles, it starts to break down into water and oxygen. The chemical reaction continues until the hydrogen peroxide is exhausted. To observe the system while the reaction is in progress, we image it within a few minutes of preparation.

We prepare the droplets by first adding hydrogen peroxide (Electron Microscopy Sciences, 30% v/v) to the suspension of Janus and tracer particles to make up a solution at 3% v/v hydrogen peroxide. This concentration is small enough to prevent rapid formation of oxygen bubbles, but high enough to produce active motion. All of the samples we discuss have either 0% (unpowered) or 3% (powered) hydrogen peroxide. We then combine 15  $\mu\text{L}$  of this aqueous solution with 60  $\mu\text{L}$  of fluorinated oil (HFE-7500, 3M Novec) containing 2% w/w surfactant (008-FluoroSurfactant, Ran Biotechnologies, Beverly, MA) and vortex this mixture for 30 to 60 s. The resulting water-in-oil emulsion contains water droplets with diameters between about 20 and 80  $\mu\text{m}$  (Figure 1D). We use this particular combination of ingredients because the fluorinated oil and surfactant prevent the particles from adhering to the interface of the droplets [6], thus allowing them to move about the droplet interior.

To observe the droplets under the microscope, we pipette 6  $\mu\text{L}$  of the emulsion onto an open-top platform prepared by epoxying a metal washer to a glass coverslip. The exposed top surface allows oxygen bubbles from the chemical reaction to escape the sample. We then immediately place the sample on an inverted microscope (Nikon TE2000) with a  $60\times$  water-immersion objective (CFI Plan Apo, Nikon) and  $1.5\times$  tube lens for fluorescence imaging.

## 2.5 Recording the particle motion

Using the microscope chamber described above, we record fluorescence images of Janus particles and passive tracer particles in the aqueous droplets (Figure 2A). The aqueous droplets float in fluorinated oil. We image through the oil to the lowest droplets, furthest from the emulsion-air interface, where evaporation of the oil and water can cause droplets to move. We fluorescently image the two types of dyed particles simultaneously with an LED illuminator (Spectra-X light engine, Lumencor, Beaverton, OR) and a multiband filtercube (DA/FI/TR/Cy5-A-NTE, Semrock, Rochester, NY). We collect AVI videos using a color camera (DCC3240C, Thorlabs, Newton, NJ) and associated software. With this widefield technique, we observe only those particles that are close to the focal plane.

## 2.6 Tracking particle trajectories

To analyze the motion of the two species of particles, we first use the Fiji distribution of the ImageJ software package [7] to separate the images into red and green files (Figure 2) based on the color channel of the camera. Although some fluorescence bleeds into the opposite channel, it is faint enough to remove with an appropriate choice of threshold. After applying the threshold, we can clearly distinguish Janus particles from tracer particles. We use the Python library Trackpy (<https://soft-matter.github.io/trackpy>) [8] to locate the centroids of the particles in each pre-processed frame and to link the coordinates of these particles together into trajectories.

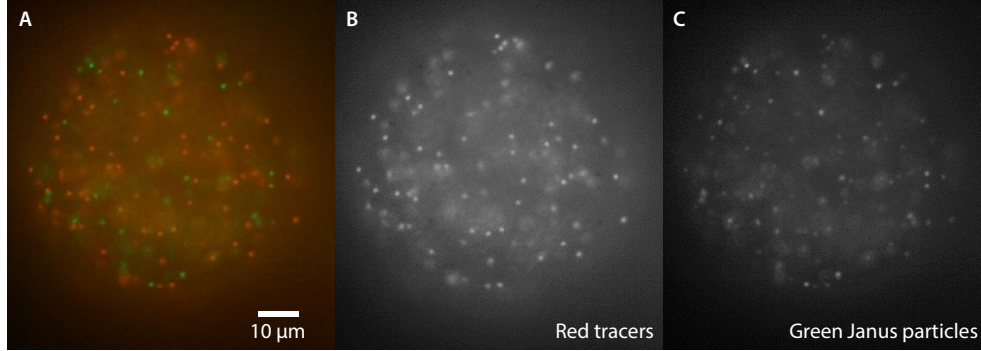


Figure 2: Red tracer particles and green Janus particles are encapsulated in an aqueous droplet (70  $\mu\text{m}$  diameter), which serves as our simplified model of an artificial cell (A). We analyze the red channel to track the tracer particles (B) and the green channel to track the Janus particles (C).

## 2.7 Subtracting rotational and translational drift

We calculate the overall drift of the droplets to separate the random motion within the droplets from the coherent motion of the droplets themselves. We use a singular value decomposition (SVD) method [9] to model the three-dimensional rigid-body rotation and translation of the droplet, based on the two-dimensional particle trajectories. The rotation is calculated about a different axis for each time step, and the rotational and translational drift is subtracted from the trajectories to obtain the motion in the droplet frame.

# 3 Results

## 3.1 Observations of system

As shown by the microscope images in Figure 2, we are able to create stable emulsion droplets with the two types of particles and the hydrogen peroxide. The particles do not aggregate in the interior of the droplets, and we do not observe them adhering to the interface.

## 3.2 Droplet motion affects particle trajectories

We observe large-scale translational and rotational motion of our droplets that most likely arises from growing oxygen bubbles. Although translational drift is a common problem in particle tracking experiments, the bulk rotational motion is especially problematic in the droplet system, since each droplet can rotate independently. The effects of the bulk motion can be seen in the trajectories of the Janus particles in Figure 3A, which show an elongation that corresponds to a large-scale motion of the droplet, likely arising from forces external to it.

To correct for this effect, we calculate the rotational and translational drift as described in the Methods section, and we subtract it from the particle trajectories. The resulting trajectories, shown in Figure 3B, explore a smaller area with less elongation.

To determine whether the drift subtraction artificially reduces the measured, powered motion of the Janus particles, we calculate the speed distribution of the Janus particles before and after drift subtraction (Figure 3C). The speed is calculated from the displacement  $\Delta r$  in the focal plane measured over the interval between frames and divided by the frame interval. The ensemble drift

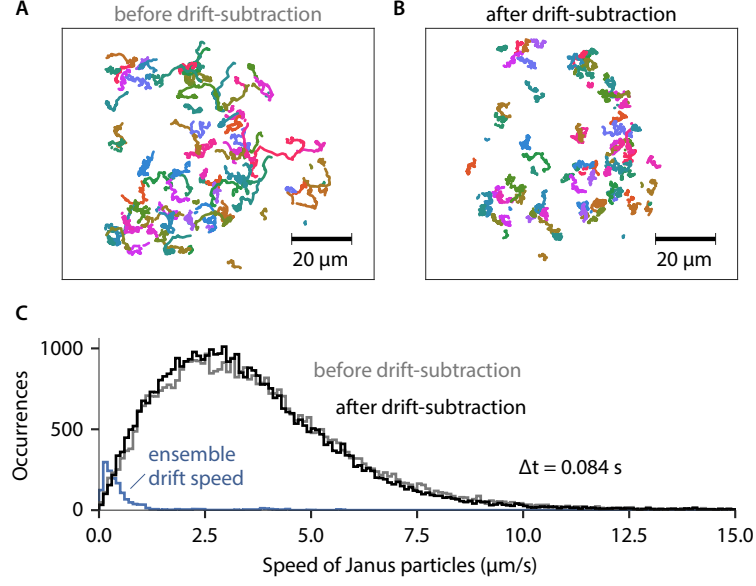


Figure 3: We track powered Janus particles in an emulsion droplet. Prior to any drift subtraction (A), the trajectories show evidence of correlated motion arising from translation and rotation of the droplet. After drift subtraction (B), there is less correlated motion, and we observe the particles exploring a smaller area. These trajectories are selected from the portion of the video sequence that showed the largest translational drift, so as to illustrate the effect clearly; in most cases the drift is not so easily discerned by eye. C: Speed distributions of Janus particles before (gray) and after (black) drift subtraction, compared to the distribution of translational drift speeds (blue). The plot shows that the Janus particles move faster than the ensemble-averaged drift speed. Thus, while drift subtraction removes the correlated motion of particles arising from movement of the droplet, we do not expect it to remove the powered motion of the Janus particles themselves. All speeds are measured in the focal plane of the droplet shown in Figure 2. The areas of the histograms differ because the number of data points for the ensemble is the number of frames in the trajectory, while the number of data points in the particle histograms is the number of frames times the number of particles in each frame.

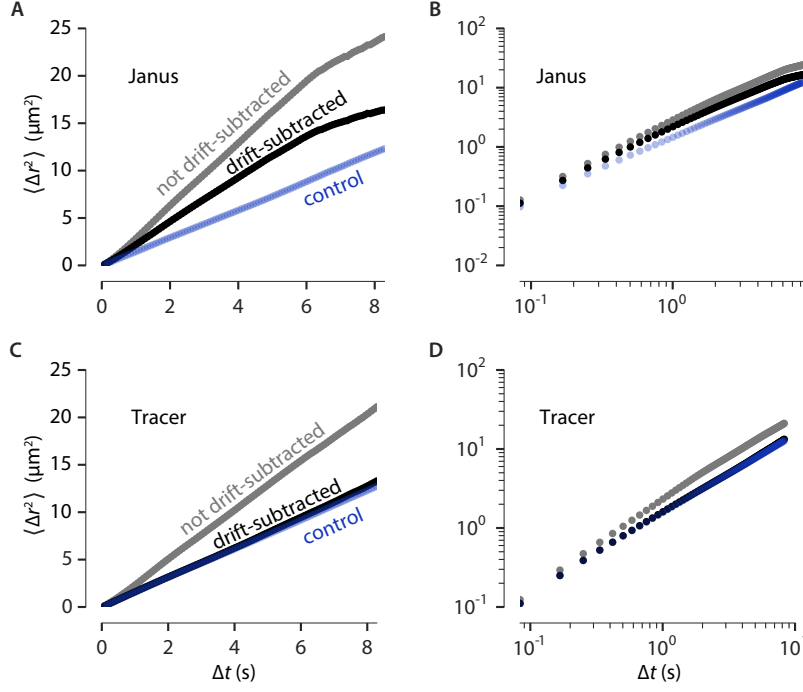


Figure 4: The ensemble mean square displacements (MSD)  $\langle \Delta r^2 \rangle$  of both active Janus (A,B) and tracer particles (C,D) in the same droplet as a function of lag time  $\Delta t$ . The two-dimensional ensemble MSD is shown both before (gray) and after (black) drift-subtraction. The log-log plots at right (B,D) show the same datasets as the left (A,C). A control sample lacking hydrogen peroxide (blue) is shown for comparison.

speed is the ensemble-average displacement  $\sqrt{\langle \Delta x \rangle^2 + \langle \Delta y \rangle^2}$  for each frame, again divided by the interval between frames. We see that the ensemble-average speed is peaked at  $0.2 \mu\text{m/s}$  with a mean of  $0.65 \mu\text{m/s}$  and median of  $0.34 \mu\text{m/s}$ . The speed of the Janus particles is peaked at  $2.5 \mu\text{m/s}$  with a mean of  $3.7 \mu\text{m/s}$  and median of  $3.3 \mu\text{m/s}$  before subtraction and a mean of  $3.6 \mu\text{m/s}$  and median of  $3.2 \mu\text{m/s}$  after subtraction. The drift correction therefore does not significantly affect the measured motion of the particles at short times, because the drift velocity is small compared to the velocity of the particles.

We also characterize the motion by calculating the ensemble-average MSD, and we compare it to that measured in a control experiment, where we use droplets containing both types of particles but do not add any hydrogen peroxide (Figure 4). For both Janus particles and tracers, the drift subtraction reduces the apparent MSD at all lag times, as expected. The MSD becomes smaller because the drift is not random. Instead, the motion of the droplet is correlated over many frames. This effect, if left uncorrected, would lead to a spuriously large MSD for both the Janus particles and tracers.

The drift-corrected MSDs show two features that we discuss in the next two subsections. First, the Janus particles have a higher MSD at all lag times than they do in the absence of hydrogen peroxide (Figure 4A), and the MSD on a log-log plot has a larger slope (Figure 4B). This enhancement persists even after drift subtraction. Second, the drift correction brings the MSD of the tracer particles in hydrogen peroxide much closer to that of the particles in the absence of hydrogen peroxide (Figure 4C–D).

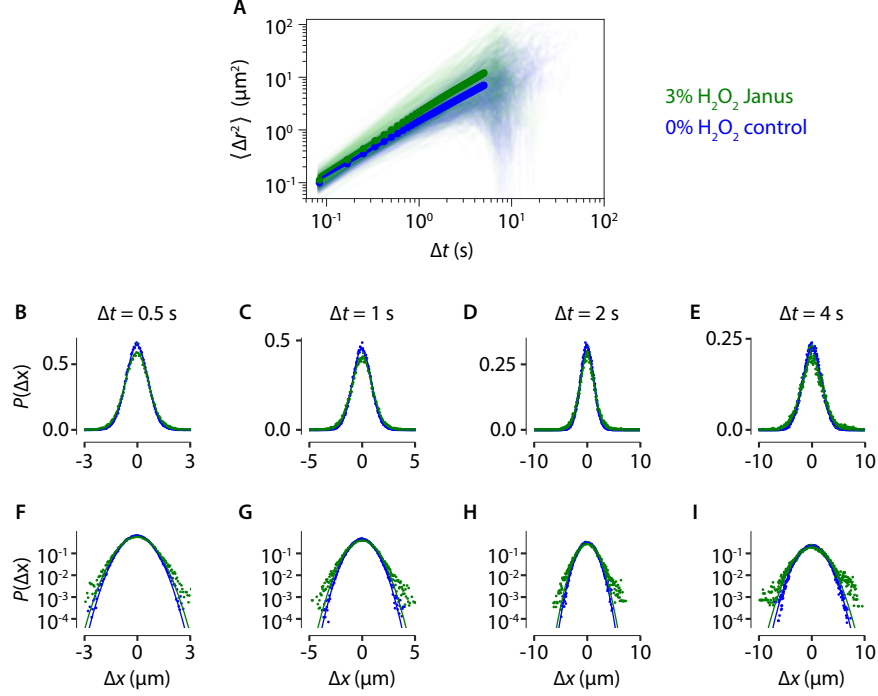


Figure 5: (Color online) Janus particles move superdiffusively in an emulsion droplet in the presence of hydrogen peroxide. A: Ensemble mean square displacement (MSD) as a function of lag time. The light traces show the MSD for individual particles, to indicate the spread of particle MSDs. The ensemble MSD log plot shows a greater slope for the powered Janus particles than the unpowered Janus particles, characteristic of superdiffusive motion. We fit the data up to 8.4 s, because the noise is high at larger lag times, as shown by the spread of the traces (note that the noise appears uneven because the MSD is plotted on a log scale). B-D: Plots of the displacement distribution of powered (green) and unpowered (blue) Janus particles at lag times of 0.5 s (B), 1 s (C), 2 s (D), and 4 s (E). F-I: the same distributions shown on log-linear axes. The trajectories for these plots are drift-subtracted.

### 3.3 Janus particles show enhanced diffusion in droplets

The larger amplitude and slope of the MSD of the Janus particles (after drift correction) relative to those of control particles suggest that the particles are in fact being driven by the breakdown of the hydrogen peroxide fuel. Further evidence for powered motion is shown in Figure 5, which shows the displacement distributions for Janus particles as a function of lag time both with and without hydrogen peroxide. Diffusive particles show Gaussian distributions (Figure 5B–E), as expected, with widths corresponding to the ensemble mean square displacement (Figure 5A). The log plots (Figure 5F–I) reveal that the distribution of the active Janus particles diverges from a Gaussian, with larger-than-expected probability for a portion of the population of Janus particles to travel more than 4  $\mu\text{m}$  in 1 s.

We first fit the MSD using a model of the form  $\Delta r^2 = A\Delta t^n$ , where  $\Delta r^2$  is the two-dimensional MSD,  $\Delta t$  is the lag time,  $A$  is a prefactor, and  $n$  is an exponent. We find that for the unpowered particles  $n = 1.00 \pm 0.03$ , and for the powered particles  $n = 1.10 \pm 0.05$ , about 10% higher. We estimate the uncertainty in the fitting parameters by considering the variation among individual

particles. A typical standard error from the fit cannot be used because the data at different lag times are correlated.

An exponent larger than 1.0, such as we observe here, shows that the powered Janus particles move superdiffusively. Previous experiments and theoretical models [10, 11] have shown that Janus particles move ballistically at short timescales (with an exponent of 2) and diffusively at longer timescales (with an exponent of 1). The non-Gaussianity we observe in the displacement distributions is further evidence that the particles are in the superdiffusive regime. Similar non-Gaussian behavior has been observed and described theoretically by Zheng and coworkers [10] for catalytic Janus particles in bulk. The origin of the non-Gaussian behavior is the ballistic motion of the particles, which does not lead to random-walk motion on these timescales. An exponent of 1.10 suggests that our observations of the motion may be in a region of timescales between the ballistic and diffusive regimes, but closer to the diffusive.

At long timescales, we expect the diffusion to be enhanced. Because we are close to this long-timescale diffusive regime, we fit the MSD to a diffusion model,  $\Delta r^2 = 4D\Delta t$ , where  $D$  is the apparent diffusion coefficient. We find that for the unpowered Janus particles,  $D = 0.3513 \pm 0.0002 \mu\text{m}^2/\text{s}$ . The value for the unpowered particles is close to that measured for tracer particles in the absence of fuel (see next subsection), as expected, though it is slightly lower than the Stokes-Einstein estimate  $D = 0.48 \mu\text{m}^2/\text{s}$  for a 1- $\mu\text{m}$ -diameter particle in water at 25°C, perhaps because the actual diameter of the particles is larger than 1  $\mu\text{m}$ .

The diffusion coefficient for the powered Janus particles is  $D = 0.5007 \pm 0.0016 \mu\text{m}^2/\text{s}$ , more than 40% higher than that for the unpowered particles. This result suggests that, on the timescales that we observe the motion, the particles are close to the enhanced diffusion regime. We say “close to” because the exponent of 1.10 and the displacement distributions in Figure 5 indicate that there is still some ballistic motion on these timescales.

### 3.4 Motion of Janus particles and tracers is weakly coupled

Having shown that the Janus particles are actively driven, even inside the emulsion droplets, we now examine the coupling between the Janus particles and the tracer particles. An analysis of the displacement distributions (Figure 6) at different lag times shows little difference between tracer particles in droplets with powered Janus particles and tracer particles in droplets not containing fuel. In both cases, the displacement distribution is Gaussian, and the widths of the Gaussians with and without fuel are nearly identical. A fit to a diffusion model,  $\Delta r^2 = 4D\Delta t$ , where  $D$  is the apparent diffusion coefficient, yields  $D = 0.3880 \pm 0.0003 \mu\text{m}^2/\text{s}$  for tracers in the presence of powered Janus particles, and  $D = 0.3816 \pm 0.0002 \mu\text{m}^2/\text{s}$  for tracers in the presence of unpowered Janus particles. Though there is a statistically significant difference between the two diffusion coefficients, it is small (less than 2%). Thus, even though the Janus particles show enhanced diffusion, the tracer particles show much smaller enhancement, indicating that the motion of the two types of particles is weakly coupled.

## 4 Discussion

Our results show that Janus particles can exhibit enhanced diffusion inside a confined system. The enhancement is evidenced by a 40% increase in the diffusion coefficient at lag times of approximately 1 s. The exponent of the mean square displacement is approximately 1.10 at these lag times, indicating that there is still some observable ballistic motion at these timescales. In the established physical picture of how active particles move [12], the enhanced diffusion regime arises

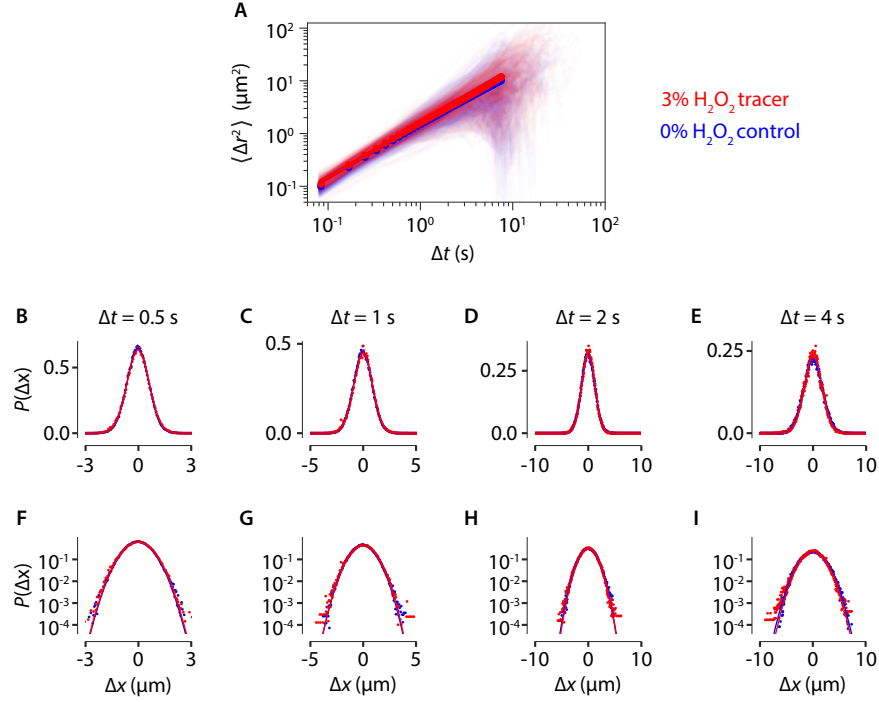


Figure 6: (Color online) The motion of tracer particles is weakly coupled to that of powered Janus particles. A: Ensemble mean square displacement (MSD) of the tracer particles as a function of lag time. Red data is for particles in the presence of Janus particles and hydrogen peroxide. Blue data is for particles in the presence of Janus particles but without hydrogen peroxide. The light traces show the MSD for individual particles, to indicate the spread of particle MSDs. B–E: Plots of the displacement distribution  $P(\Delta x)$  of tracer particles in the presence of powered Janus particles (red) and in the presence of unpowered Janus particles (blue) Janus at lag times of 0.5 s (B), 1 s (C), 2 s (D), and 4 s (E). F–I: the same distributions shown on log-linear axes. The trajectories for these plots are drift-subtracted.

from powered, ballistic motion at short time scales combined with rotational diffusion at longer timescales, which randomizes the direction of the ballistic motion.

Following Zheng and coworkers [10], we calculate the timescale at which we expect the transition from ballistic motion to enhanced diffusion to begin. This timescale is  $t = 1/(2D_r)$ , where  $D_r$  is the rotational diffusion coefficient, which is approximately  $1 \text{ s}^{-1}$  for our system. We find  $t \approx 0.5 \text{ s}$ , which is just below the range of lag times (1–4 s) at which we observe the enhanced diffusion. Thus, the observation of enhanced diffusion (and the slightly superdiffusive exponent) make sense in the context of this theoretical framework: We are observing the motion at timescales slightly larger than the transition time, so that we see enhanced diffusion along with some residual ballistic motion, which is apparent in the displacement distributions.

However, the activity of the Janus particles does not seem to enhance the diffusion of the tracers. There are several possible reasons for the lack of coupling between the motion of the two types of particles. First, the coupling between particles is hydrodynamic, and because the Janus particles are active, they act as force dipoles [12]. The velocity in the far field therefore decays with distance  $r$  as  $1/r^2$ , compared to  $1/r$  for an externally driven flow field [13]. Therefore, at the low volume fractions we use, the hydrodynamic coupling might be weak. Furthermore, the magnitude of the force dipole might also be small for our system, because we use low concentrations of hydrogen peroxide in order to delay bubble formation.

Second, the efficiency of conversion of chemical energy to directed motion is many orders of magnitude smaller for catalytic micromotors such as our Janus particles than for molecular motors [14]. A more efficient active particle would likely show a larger force dipole and stronger coupling to the tracer particles.

Third, in living cells the cytoplasm is crowded with proteins and filaments, making it a weak elastic gel [1]. In cells depleted of ATP, passive tracer particles show very small mean square displacements [1], indicating that they are trapped by the elasticity of the medium. The enhanced diffusion of the tracer particles in the presence of ATP-driven motor activity is therefore due to the nonlinear elastic properties of the medium. By contrast, the fluid inside the droplets in our system is purely viscous and linear.

These considerations suggest several future directions for making an improved model system for mimicking transport inside the cytoplasm. For example, one might increase the concentration of the motor particles. However, a higher concentration of Janus particles would rapidly deplete the hydrogen peroxide and increase the rate of bubble formation. An alternative approach is to use biological motors instead of synthetic ones, since their efficiency is orders of magnitude higher than that of the Janus particles. Bacterial baths are a useful point of comparison: many studies have shown that the diffusion of tracer particles is significantly enhanced—by a factor of two or more—in three-dimensional suspensions of motile *E. coli* bacteria at volume fractions of active particles comparable to [15, 16] or even smaller [17] than ours (1%). The reason for the stronger coupling may be that the efficiency, and hence the force dipole, is much larger for a bacterium than for a catalytic Janus particle.

If one wanted to use synthetic motors, light-driven Janus particles [12] might be preferable, since they circumvent the problem of bubble formation. However, the binary liquid mixture needed for such particles might not be compatible with the emulsion system we show here, and a different method of confinement might be required.

With our current system of catalytic Janus particles, it would be interesting to investigate the effects of crowding and elasticity of the medium. Although the Janus particles have a weak effect on the motion of tracer particles within a viscous medium, they might have a much larger effect on particles in a weak elastic gel, because the thermally driven diffusion of the tracer particles within the gel would be very small.

## 5 Conclusion

We have shown that active Janus particles, passive tracer particles, and chemical fuel (hydrogen peroxide) can be confined within emulsion droplets, such that the Janus particles show enhanced diffusion and do not stick to the droplet interfaces. In these experiments we are careful to correct for bulk rotational and translational motion induced by bubble formation. After this correction we find that the motion of the passive tracer particles is weakly coupled to that of the active Janus particles, likely because the efficiency and concentration of the Janus particles is too low. Nonetheless, the results point the way forward toward a model system that can be used to understand active transport in living cells, where the motion of motors can significantly enhance the diffusion of unattached particles within the cytoplasm. Future versions of such a system might benefit from introducing crowding agents or more efficient active particles. If diffusion-limited chemical reactions can be sped up by the particles, it might enable the use of artificial cells as biochemical factories.

## Acknowledgments

We acknowledge support from the Army Research Office through the MURI program under award no. W911NF-13-1-0383, from the Harvard Materials Research Science and Engineering Center through NSF grant no. DMR-1420570, and from the Swedish Research Council (Vetenskapsrådet) 637-2013-414. We thank Ilona Kretzschmar, Sepideh Razavi, and Bin Ren for guidance in making Janus particles and W. Benjamin Rogers and Kinneret Keren for helpful discussions. This work was performed in part at the Harvard Center for Nanoscale Systems (CNS), a member of the National Nanotechnology Infrastructure Network (NNIN), which is supported by the NSF (ECS-1541959).

## Author contributions

V.R.H., T.G.D., and V.N.M. conceived of the presented idea. Z.C.C. prepared samples and collected data. V.R.H., Z.C.C., and V.N.M. performed analysis. İ.G. developed the method for making Janus particles and contributed diagrams. V.R.H., T.G.D., İ.G., and V.N.M. wrote the paper. All authors gave final approval for the paper to be published.

## Data availability

The datasets generated during the current study are available from the corresponding author on reasonable request.

## References

- [1] M. Guo, A.J. Ehrlicher, M.H. Jensen, M. Renz, J.R. Moore, R.D. Goldman, J. Lippincott-Schwartz, F.C. Mackintosh, D.A. Weitz, *Cell* (2014), **158**, 822
- [2] J.C. Crocker, B.D. Hoffman, in *Cell Mechanics*, edited by Y.L. Wang, D. Discher (Elsevier Academic Press, San Diego, 2007), Vol. 83 of *Methods in Cell Biology*, pp. 141–178
- [3] J.R. Howse, R.A.L. Jones, A.J. Ryan, T. Gough, R. Vafabakhsh, R. Golestanian, *Physical Review Letters* (2007), **99**, 048102
- [4] S. Wang, N. Wu, *Langmuir* (2014), **30**, 3477
- [5] A. Brown, W. Poon, *Soft Matter* (2014), **10**, 4016

- [6] C. Holtze, A.C. Rowat, J.J. Agresti, J.B. Hutchison, F.E. Angilè, C.H.J. Schmitz, S. Köster, H. Duan, K.J. Humphry, R.A. Scanga et al., *Lab on a Chip* (2008), **8**, 1632
- [7] J. Schindelin, I. Arganda-Carreras, E. Frise, V. Kaynig, M. Longair, T. Pietzsch, S. Preibisch, C. Rueden, S. Saalfeld, B. Schmid et al., *Nature Methods* (2012), **9**, 676
- [8] D. Allan, T.A. Caswell, N. Keim, F. Boulogne, R.W. Perry, L. Uieda, Zenodo doi: 10.5281/zenodo.34028 (2015)
- [9] P.J. Besl, N.D. McKay, *IEEE Transactions on Pattern Analysis and Machine Intelligence* (1992), **14**, 239
- [10] X. Zheng, B. ten Hagen, A. Kaiser, M. Wu, H. Cui, Z. Silber-Li, H. Löwen, *Physical Review E* (2013), **88**, 032304
- [11] J. Palacci, C. Cottin-Bizonne, C. Ybert, L. Bocquet, *Physical Review Letters* (2010), **105**, 088304
- [12] C. Bechinger, R. Di Leonardo, H. Löwen, C. Reichhardt, G. Volpe, G. Volpe, *Reviews of Modern Physics* (2016), **88**, 045006
- [13] E. Lauga, T.R. Powers, *Reports on Progress in Physics* (2009), **72**, 096601
- [14] W. Wang, T.Y. Chiang, D. Velegol, T.E. Mallouk, *Journal of the American Chemical Society* (2013), **135**, 10557
- [15] M.J. Kim, K.S. Breuer, *Physics of Fluids* (2004), **16**, L78
- [16] L.G. Wilson, V.A. Martinez, J. Schwarz-Linek, J. Tailleur, G. Bryant, P.N. Pusey, W.C.K. Poon, *Physical Review Letters* (2011), **106**, 018101
- [17] D.T.N. Chen, A.W.C. Lau, L.A. Hough, M.F. Islam, M. Goulian, T.C. Lubensky, A.G. Yodh, *Physical Review Letters* (2007), **99**, 148302